

Interleukin-6 prevents NMDA-induced neuronal death via Gp130 signaling-dependent IP3R inhibition

Ao-Wang QIU*, Qin YANG*, Song-Tao YUAN, Ping XIE, Qing-Huai LIU

Department of Ophthalmology, The First Affiliated Hospital with Nanjing Medical University, 300 Guangzhou Road, Nanjing, Jiangsu Province 210029, China

* Authors contributed equally to this study

Correspondence to: Qing-Huai Liu
Department of Ophthalmology,
The First Affiliated Hospital with Nanjing Medical University,
300 Guangzhou Road, Nanjing, Jiangsu Province 210029, China.
E-MAIL: qinghuailiu@163.com

Submitted: 2013-05-21 Accepted: 2013-09-12 Published online: 2013-11-25

Key words: interleukin-6; neuronal apoptosis; neuronal necrosis; inositol 1,4,5-trisphosphate receptors; ryanodine receptors; gp130

Neuroendocrinol Lett 2013; 34(6):529–538 PMID: 24378454 NEL340613A09 © 2013 Neuroendocrinology Letters • www.nel.edu

Abstract

OBJECTIVE: To reveal the involvement of inositol 1,4,5-trisphosphate receptors (IP3R) and ryanodine receptors (RyR) in IL-6 prevention from neuronal apoptosis and necrosis induced by N-methyl-D-aspartate (NMDA).

METHODS: Cerebellar granule neurons (CGNs) from 8-day-old rats were exposed to IL-6 for 8 days and then stimulated with NMDA for 30 min. The 2-aminoethoxydiphenyl borate (2-APB) and dantrolene (DAN) were used to antagonize IP3R and RyR, respectively. Anti-gp130 monoclonal antibody (mAb) was employed to neutralize gp130, a 130-kDa signal-transducing β -subunit of IL-6 receptor complex. Neuronal apoptosis and necrosis were determined by TUNEL, fluorometric caspase-3 enzyme activity, annexin V-FITC/PI staining and ELISA. Western blot and real-time PCR measured IP3R1 and RyR2 expression, respectively.

RESULTS: IL-6 prevented the elevation of TUNEL-positive cells and caspase-3 expression and activity, and also suppressed the increase in annexin V-FITC/PI-positive cells and DNA- and histone-associated nucleosomes in cultured CGNs evoked by NMDA. These anti-apoptotic and anti-necrotic effects of IL-6 were larger on DAN-treated cells than on 2-APB-exposed neurons, since 2-APB treatment alone significantly inhibited the neuronal apoptosis and necrosis but DAN exposure alone did not alter the apoptosis and necrosis induced by NMDA. In support of these results, IL-6 downregulated IP3R1 but did not affect RyR2 expression. All these IL-6 effects were blocked by anti-gp130 mAb.

CONCLUSION: IL-6 prevention from NMDA-triggered Ca^{2+} -induced Ca^{2+} release-mediated apoptosis and necrosis in CGNs depends on the inhibition of IP3R channel opening and expression rather than on RyR activity. IL-6 receptor-coupled gp130 signaling mediates this neuroprotection of IL-6 resistance to neuronal apoptosis and necrosis.

INTRODUCTION

Interleukin-6 (IL-6), a cytokine that is involved in induction, growth and differentiation of cells in the immune and hematopoietic systems, is also found in the brain. IL-6 in the brain is produced not only by the innate immune cells, microglia and astrocytes, but also by neurons (Schöbitz *et al.* 1992; Schöbitz *et al.* 1993). In many brain regions, such as the hippocampus, habenular nucleus, hypothalamus, and cerebral and cerebellar cortices, neurons express IL-6 and IL-6 receptors (Gadient & Otten 1993, 1994), suggesting an involvement of IL-6 in modulation of neuronal activity. In normal state of the brain, IL-6 level is low, but it is greatly elevated in brain infection, injury and diseases, such as viral meningitis, ischemia, trauma, epilepsy, amyotrophic lateral sclerosis, Alzheimer's and Parkinson's diseases (Frei *et al.* 1988; Laurenzi *et al.* 1990; Arundine & Tymianski 2003; Cucchiaroni *et al.* 2010; Dalla *et al.* 2011). The elevated IL-6 may represent a mechanism mediating the brain infection, injury or diseases, but also may reflect a compensatory protection against further pathological changes in brain. Some studies *in vivo* and *in vitro* have indicated that IL-6 has neuroprotective effect (Erta *et al.* 2012). As expected, IL-6 is upregulated in several animal models of brain injury and shows a myriad of actions as suggested by studies in IL-6 KO mice which show a compromised inflammatory response, increased oxidative stress, impaired neuroglial activation, decreased lymphocyte recruitment and a slower rate of recovery and healing (Klein *et al.* 1997; Penkowa *et al.* 2000; Galiano *et al.* 2001; Swartz *et al.* 2001). In line with the results with IL-6 KO mice, GFAP-IL-6 mice that overexpress IL-6 in the brain shows more rapid healing and recovery after traumatic brain injury (Swartz *et al.* 2001; Penkowa *et al.* 2003). In the studies *in vitro*, IL-6 promotes survival of cultured basal forebrain and septal cholinergic neurons, mesencephalic catecholaminergic neurons (Hama *et al.* 1989, 1991), and retinal ganglion cells (Mendonça *et al.* 2001). A survival mechanism is related to the inhibition of glutamate excitotoxicity, as IL-6 limits neurotoxic effect produced by retinal injection of N-methyl-D-aspartate (NMDA) (Inomata *et al.* 2003) and IL-6 protects cultured cerebellar granule neurons (CGNs) against excitotoxicity induced by glutamate or NMDA (Peng *et al.* 2005; Wang *et al.* 2009; Liu *et al.* 2011). However, IL-6, as a versatile cytokine, plays a neurotrophic, neuroprotective or neurotoxic role, depending on conditions (Suzuki *et al.* 2009; Spooren *et al.* 2011; Erta *et al.* 2012). For example, GFAP-IL-6 mice also show a diminished hippocampal neurogenesis (Vallieres *et al.* 2002), and *in vitro* IL-6 decreases the differentiation of neural stem/progenitor cells into neurons (Monje *et al.* 2003; Nakanishi *et al.* 2007). Thus, mechanisms underlying IL-6 action need to be further explored to better understand IL-6 effect and to provide more targets for therapeutic strategy of brain infection, injury and diseases.

Neuronal injury and death are closely associated with intracellular Ca^{2+} levels. NMDA-evoked intracellular Ca^{2+} overload is a major factor leading to excitotoxicity, by which neuronal apoptosis and necrosis occur in acute and chronic brain injuries and diseases. NMDA-induced intracellular Ca^{2+} overload involves several mechanisms, including Ca^{2+} influx through NMDA-gated receptor channels, Ca^{2+} influx through voltage sensitive Ca^{2+} channels activated by membrane depolarization and Ca^{2+} release from intracellular Ca^{2+} stores. The Ca^{2+} release is induced by high cytosolic Ca^{2+} as a result of extracellular Ca^{2+} influx and therefore, it is termed Ca^{2+} -induced Ca^{2+} release (Gruol *et al.* 2010; Popescu *et al.* 2010). In neurons, the endoplasmic reticulum also serves as a Ca^{2+} store and it releases Ca^{2+} into cytosol via Ca^{2+} channel receptors located on membrane of this organelle, including inositol 1,4,5-trisphosphate receptors (IP3R) and ryanodine receptors (RyR) (Verkhratsky & Petersen 2002). A report has shown that IL-6 suppression of NMDA-triggered Ca^{2+} release from the Ca^{2+} stores is more important than its suppression of Ca^{2+} influx through NMDA receptors (Sun *et al.* 2011). Nevertheless, respective contribution of the two kinds of Ca^{2+} channel receptors, IP3R and RyR, to IL-6 neuroprotection still remains to be clarified.

It is clear that excess activation of ionotropic glutamate receptors, such as NMDA receptors (NMDAR), cause influx and accumulation of Ca^{2+} and Na^{+} that result in rapid swelling and subsequent neuronal death within a few hours (Won *et al.* 2002) and that Ca^{2+} mediates cell death by reinforcing signals leading to caspase activation, by activating proteases, or by triggering other catabolic processes mediated by lipases and nucleases (Bano & Nicotera 2007). These reports have also presented that IL-6 attenuates glutamate- or NMDA-induced intracellular Ca^{2+} overload and subsequently reduces neuronal apoptosis and necrosis (Peng *et al.* 2005; Spooren *et al.* 2011), supporting a close connection between neuronal Ca^{2+} overload and death. However, direct evidence showing the relationship between IL-6 inhibition of Ca^{2+} release from the intracellular Ca^{2+} stores and the reduction of neuronal death is not provided. Thus, in the present study, we used 2-aminoethoxydiphenyl borate (2-APB) and dantrolene (DAN), the antagonists for IP3R and RyR, respectively, to block Ca^{2+} release from the intracellular Ca^{2+} stores, and then observed effect of IL-6 on NMDA-triggered neuronal apoptosis and necrosis. In addition, a neutralizing antibody to gp130, a 130-kDa signal-transducing β -subunit of IL-6 receptor complex, is employed to block IL-6 signal transduction in order to confirm the IL-6 effect.

MATERIALS AND METHODS

Cell culture preparation

Primary cultures of CGNs were obtained from dissociated cerebella of 8-day-old Sprague-Dawley rats

(Fernandez-Gomez *et al.* 2005). The cerebella were removed from the rats and minced with sterile surgical blades. The minced cerebella were chemically dissociated in the presence of trypsin and DNase I and plated in poly-L-lysine-coated (50 mg/l) wells. Cells were seeded at a density of 2.5×10^5 cells/cm² in the complete culture medium composed of BME (Sigma, USA) supplemented with 0.1 g/l gentamicin, 2.2 g/l NaHCO₃, 2.385 g/l HEPES, 25 mM KCl, and 10% heat-inactivated fetal bovine serum. The samples were incubated at 37 °C with a humidified 5% CO₂/95% air atmosphere in an incubator. Cytosine arabinoside (10 μM) was added 24 h after the cell plating to inhibit glial proliferation, and thus CGNs developed under the cultured conditions.

Drug treatment

Rat recombinant IL-6 (R&D, USA) of 120 ng/ml was added to CGN cultures on days 1, 4 and 7 (every 72 h) to keep the concentration of exogenously added IL-6 relatively constant during the period of chronic treatment. Anti-gp130 monoclonal antibody (mAb, Chemicon, USA) was added to the medium 1 h prior to IL-6 at a dose of 75 ng/ml to neutralize IL-6 signal transduction. The 2-APB or DAN (both 100 μM and from Sigma, USA) was applied to the 8-day CGN cultures 30 min prior to NMDA treatment. NMDA (Sigma, USA) was dissolved in Locke's solution, which was applied to the 8-day cultures at a concentration of 100 μM for 30 min at room temperature and then washed off. Locke's solution (pH 7.4) contained the following (in mM): 134 NaCl, 25 KCl, 2.3 CaCl₂, 4 NaHCO₃, 5 HEPES, 5 D-glucose and 0.01 glycine. The cultures were again incubated with the primary culture medium in the CO₂ incubator for 8 h for measurement of caspase-3 expression and activity and IP3R1 and RyR2 expression, or for 18 h for detection of TUNEL assay, annexin V-FITC/PI staining and ELISA.

Terminal deoxynucleotidyl transferase-mediated deoxy-UTP-fluorescein nick end labeling (TUNEL) assay

TUNEL assay was performed using In Situ Cell Death Detection Kit (Roche, Germany) according to the manufacturer's instructions. Primary CGNs (5×10^5 /well) were cultured in poly-L-lysine-coated coverslip in a 24-well plate, washed twice with PBS, and fixed with 4% PFA in PBS for 30 min at room temperature. The cells were washed three times and permeabilized with 0.1% Triton X-100 for 5 min on ice followed by incubation with TUNEL assay reagent in the dark for 1 h at 37 °C. Total cell number was determined by Hoechst33342 staining of nuclei. The cells were washed with PBS twice and TUNEL-positive cells were quantified under fluorescence microscopy. The number of apoptotic cells was counted from 5 randomly selected fields for each coverslip and mean values were from three replicates. Apoptotic rate was expressed as percentage of apoptotic cells in total cells.

Western blot analysis

For immunoblotting of caspase-3 and IP3R1 in total cell lysates, 30 μg of total protein was resolved in SDS-polyacrylamide gels and transferred onto polyvinylidene difluoride membrane using a wet Trans-Blot (Bio-Rad, USA). Membranes were blotted with rabbit antibodies specific for caspase-3 (1:200, Santa Cruz, USA) or IP3R1 (1:1 000, Millipore, USA) following the instructions of the provider. They were incubated with the IRDye 800-conjugated goat anti-rabbit IgG (1:5 000, Rockland, USA) for 1 h at room temperature. As an inner control, the membranes were re-probed with a monoclonal anti-β-actin antibody, followed by reaction with IRDye 800-conjugated goat anti-mouse IgG (1:5000, Rockland, USA). Blots were developed using Odyssey laser scanning system (LI-COR, Inc., USA). Band intensity was estimated densitometrically by an image analysis system (Odyssey 3.0 software, USA).

Fluorometric caspase-3 enzyme activity assay

Caspase-3 activity in total cell lysates was determined by a fluorometric immunosorbent enzyme assay kit (Roche, Germany) using 7-amido-4-trifluoromethylcoumarin-derived substrate Ac-DEVD-AFC, according to the manufacturer's instructions. Briefly, after treated with various drugs, the cells were harvested using trypsinization and the cell lysates were seeded into a standard white 96-well plate that was pre-coated with anti-caspase-3 antibody. The plate was incubated for 1 h at 37 °C avoiding direct light. Then, Ac-DEVD-AFC, a fluorogenic substrate for caspase-3, was added to each well and the plate was incubated for 2 h at 37 °C in the dark. The assay conditions were standardized and therefore, they ensured that the products of the reaction remained in the linear range of detection. The protease activity was quantified by a multi-mode microplate reader (BioTek, USA) using 400/528 nm excitation/emission wavelengths and the sample readings were calculated by subtracting the absorbance of blank samples.

Annexin V-FITC/propidium iodide (PI) staining

Annexin V-FITC has a high affinity with phosphatidylserine that is translocated to cell surface soon after initiating apoptosis and stained into green. PI is impermeable to intact membrane and only enters necrotic cells, binding tightly to the nucleic acids in the cells and showing red fluorescence. CGNs were seeded at a density of 5×10^5 cells/well into 24-well plates. After treated with various drugs, the cells were incubated with annexin V-FITC and PI (Roche, Germany) for 15 min in the dark at room temperature. Following the labeling procedures, the cells were placed on laser scanning confocal microscope (LSCM, Leica TCS SP2, Germany). Fluorescent images of neurons were captured simultaneously by two PMT's, set for PI (>590 nm) and FITC (500–550 nm) emission wavelength ranges. Apoptotic cells that had bound annexin V-FITC alone showed

green fluorescence in the plasma membrane. Necrotic cells that had lost membrane integrity showed red fluorescence throughout the nucleus and in some cases showed the yellow due to incorporating both PI and annexin V-FITC staining.

Enzyme-linked immunosorbent assay (ELISA) for cell death detection

Cell Death Detection ELISA^{PLUS} kit (Roche, Germany), a sandwich enzyme immunoassay-based method, was employed to detect neuronal apoptosis and necrosis according to manufacturer's specifications. Mouse monoclonal antibodies against DNA and histones were used to recognize released nucleosomes after DNA nucleosomal fragmentation. CGNs were seeded in 96-well plates (Nunc, USA) at 8×10^4 cells per well. Following various treatments, the cell culture supernatants were collected and the cells were lysed with lysis buffer. The cell culture supernatants and the cell lysates were transferred to a streptavidin-coated ELISA microplate, which was incubated with anti-DNA and anti-histone antibodies for 2 h at room temperature. A peroxidase substrate was applied to produce color change, which was proportional to the amount of nucleosomes captured in the antibody sandwich. Absorbance was read on the multi-mode microplate reader at 405 nm against substrate solution as a blank (490 nm). The ELISA detection of DNA- and histone-associated nucleosomes in neuronal culture supernatants represented cell necrosis, and this detection in neuronal lysates reflected cell apoptosis.

Real-time polymerase chain reaction (PCR)

Expression of RyR2 mRNA was examined by quantitative real-time PCR. Total RNA was extracted with Trizol reagent (Invitrogen, Carlsbad, USA) according to the manufacturer's instructions. Potentially contaminating residual genomic DNA was eliminated with RNase-free DNase (Promega, Madison, USA). After the RNA content was determined by spectrophotometric analysis at 260 nm, 2 μ g of total RNA was used for cDNA synthesis with murine myelomonocytic lymphoma virus reverse transcriptase (Promega, Madison, USA). The single-stranded cDNA was then amplified. Each 20 μ l of reaction mixture contained 1 μ l of cDNA, 2 μ l PCR buffer, 3.0 mM $MgCl_2$, 0.2 mM of each dNTP, 0.2 μ M of oligonucleotide primer, and 1 U Taq DNA polymerase. Reaction procedures were set with an initial step at 95 °C for 5 min, 40 cycles of 94 °C for 30 s, 60 °C for 30 s, and 72 °C for 30 s. To verify the specificity of the amplification reaction, melting curve analysis was performed. The data were collected using the instrument's software (Rotor-Gene software, version 6.0) and relative quantification was performed using the comparative threshold method, as described by the manufacturer (User Bulletin). The sequence of PCR primer was 5'-CTACTCAGGATGAGGTGCGA-3' (sense) and 5'-CTCTCTTCAGATCCAAGCCA-3' (antisense).

Statistical analysis

Data were expressed as mean \pm standard deviation (M \pm SD). Statistical analysis was performed with Statistics Package for Social Science (SPSS, 12.0). The data were submitted to the one-way analysis of variance (ANOVA), followed by Student-Newman-Keul's test to compare all groups between each other. Differences were considered statistically significant at $p < 0.05$.

RESULTS

IL-6 reduces NMDA-induced apoptosis more in DAN-treated CGNs than in 2-APB-exposed cells, and these IL-6 effects are blocked by anti-gp 130 mAb

NMDA stimulation of cultured CGNs that had been chronically exposed to IL-6 significantly reduced percentage of TUNEL-positive cells compared with the NMDA stimulation of control neurons lacking IL-6 exposure, showing that IL-6 prevented neuronal apoptosis induced by NMDA (Figure 1). 2-APB, an antagonist of IP3R, reduced the NMDA-triggered increase in percentage of TUNEL-positive cells and IL-6 further diminished the 2-APB-dependent reduction of apoptotic cells (Figure 1). Dissimilarly, DAN, an antagonist of RyR, did not alter NMDA-triggered increase in percentage of TUNEL-positive cells, but IL-6 greatly decreased the apoptosis in DAN-treated neurons (Figure 1). Combined treatment of CGNs with IL-6 and anti-gp130 mAb, a neutralizer of gp130 that is a signal-transduction subunit of IL-6 receptors, abolished all these IL-6 effects (Figure 1).

IL-6 decreases expression and activity of caspase-3 to a larger extent in DAN-treated neurons than in 2-APB-exposed cells, and these IL-6 effects are abolished by anti-gp 130 mAb

NMDA remarkably upregulated caspase-3 expression and enhanced its activity. IL-6 prevented these changes induced by NMDA (Figure 2). 2-APB impaired the NMDA-triggered caspase-3 expression and activity, but DAN did not influence the caspase-3 changes evoked by NMDA (Figure 2). IL-6 prevented the caspase-3 changes triggered by NMDA in either 2-APB-exposed or DAN-treated neurons, but these preventive effects of IL-6 were larger on DAN-treated neurons than on 2-APB-exposed cells (Figure 2). Anti-gp130 mAb counteracted all the IL-6 preventive effects (Figure 2).

IL-6 diminishes NMDA-evoked death stronger in DAN-treated neurons than in 2-APB-treated cells, and anti-gp 130 mAb antagonizes these IL-6 effects

To show whether the mechanism underlying IL-6 prevention from neuronal apoptosis also occurred in cell necrosis, we simultaneously observed apoptotic and necrotic changes after the same treatments by annexin V-FITC/PI staining and ELISA cell death detection. The annexin V-FITC-positive cells and the DNA- and

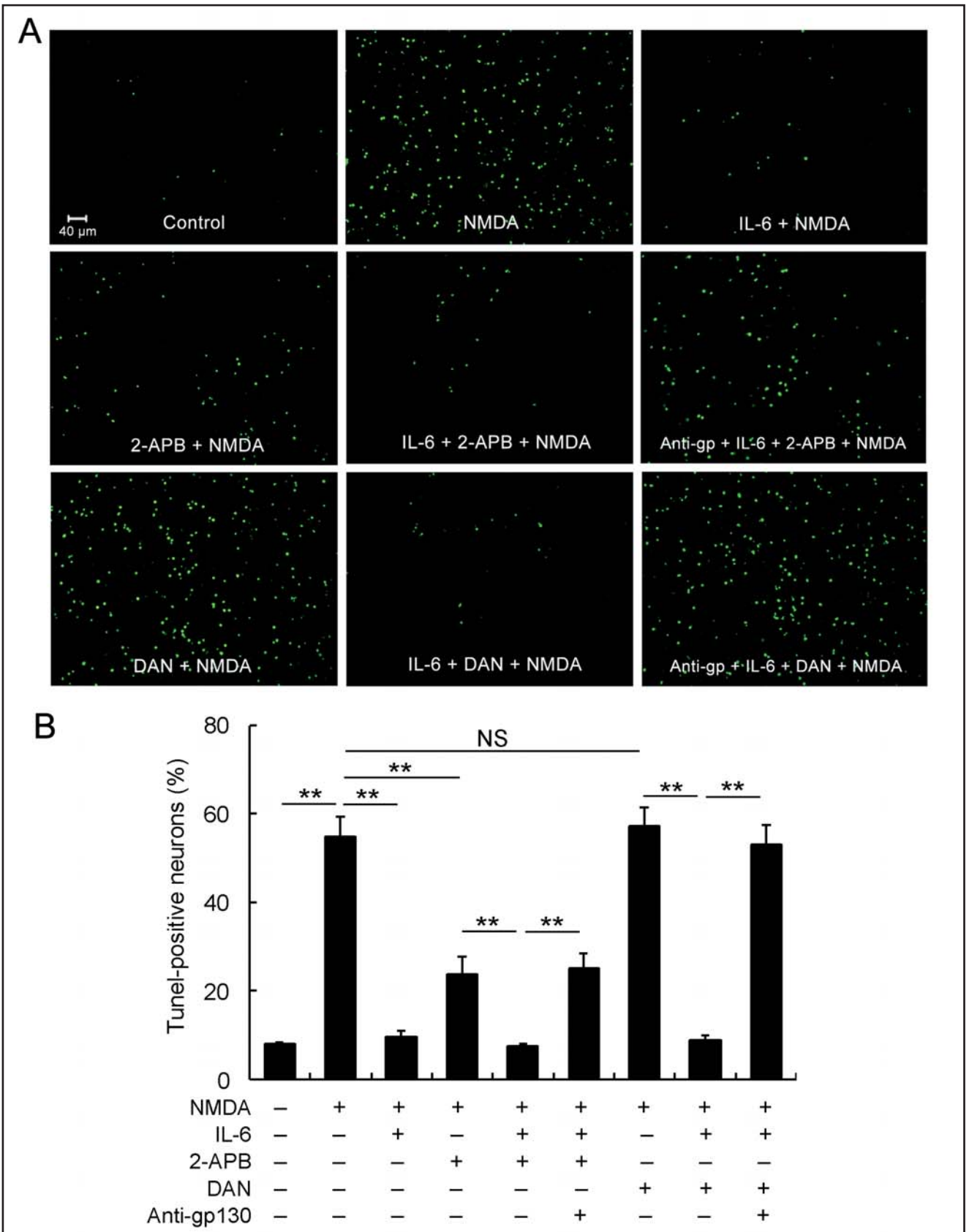


Fig. 1. Effect of IL-6 on NMDA-evoked apoptosis in 2-APB- or DAN-treated neurons. CGNs from 8-day-old rats were exposed to IL-6 (120 ng/ml) for 8 days and then stimulated with NMDA for 30 min. The 2-APB or DAN (both 100 μM) was applied to the 8-day CGN cultures 30 min prior to NMDA treatment. Anti-gp130 mAb (75 ng/ml) was added to the medium 1 h prior to IL-6. After the cultures were incubated for 18 h, TUNEL assay was performed. (A) A representative image for TUNEL-positive cells in cultured CGNs with the different treatments. (B) A statistical graph for three replicates. For each coverslip, five randomly selected fields were counted for the TUNEL-positive cells. ***p*<0.01, and NS no significance between the compared groups.

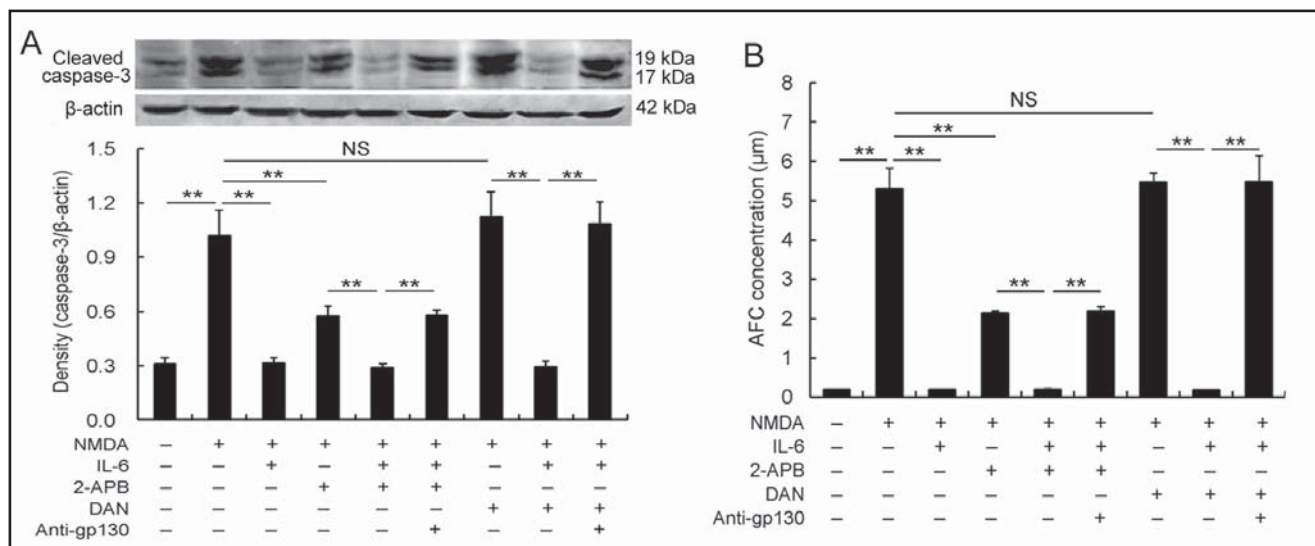


Fig. 2. Influences of IL-6 on NMDA-induced caspase-3 expression and activity in 2-APB- or DAN-treated neurons. The various treatments of CGNs were the same as designed in figure 1. The caspase-3 expression (A) and activity (B) were measured at 8 h following NMDA application by Western blot and fluorometric enzyme activity assays, respectively. The experiment was repeated for four times. $**p < 0.01$, and NS no significance between the compared groups.

histone-associated nucleosomes in cell culture lysates, which both reflected the cell apoptosis, showed that 2-APB attenuated NMDA-induced neuronal apoptosis but DAN did not affect the apoptosis (Figure 3). The preventive effect of IL-6 on neuronal apoptosis was larger in DAN-treated cells than in 2-APB-exposed cells, and anti-gp130 mAb blocked the IL-6 effects in both the conditions (Figure 3).

In addition, the increased PI-positive neurons and DNA- and histone-associated nucleosomes in cell culture supernatants induced by NMDA, which both represented neuronal necrosis, were also prevented by the IL-6 chronic exposure (Figure 3). Likewise, 2-APB reduced the NMDA-induced neuronal necrosis but DAN did not alter this elevated necrosis (Figure 3). The preventive effect of IL-6 on neuronal necrosis was stronger in DAN-treated cells than in 2-APB-exposed cells (Figure 3). Anti-gp130 mAb antagonized these IL-6 anti-necrotic effects in both DAN- and 2-APB-treated CGNs (Figure 3).

IL-6 downregulates IP3R1 but not RyR2 expression and this downregulation is counteracted by anti-gp 130 mAb

Expression of IP3R1, the most ubiquitous isoform of IP3R family, was upregulated by NMDA and this upregulation was prevented by IL-6 (Figure 4A). Anti-gp130 mAb reversed the IL-6 effect (Figure 4A). Moreover, IL-6 itself downregulated IP3R1 expression and anti-gp130 mAb also blocked this IL-6 action (Figure 4A). However, expression of RyR2, an isoform of RyR, was not influenced by any of the treatments, NMDA, IL-6, or anti-gp130 mAb (Figure 4B).

DISCUSSION

It has been well known that abnormally high level of cytosolic Ca^{2+} , such as NMDA-triggered intracellular Ca^{2+} overload, leads to cell apoptosis and necrosis. The NMDA-evoked high cytosolic Ca^{2+} , besides from extracellular Ca^{2+} influx through NMDAR located on the cytoplasmic membrane, is importantly from intracellular Ca^{2+} release through IP3R and RyR on membrane of the endoplasmic reticulum. In this study, in the cultured CGNs, apoptotic cells, reflected by TUNEL-positive cells that are determined by DNA fragmentation, was dramatically increased by NMDA application, confirming a neurotoxicity of NMDA. IL-6 prevented the NMDA-triggered neuronal apoptosis, demonstrating a neuroprotection of IL-6. Interestingly, blocking IP3R with 2-APB significantly inhibited NMDA-induced neuronal apoptosis, but blocking RyR with DAN did not alter the neuronal apoptosis. This implies that between IP3R and RyR, only IP3R-mediated Ca^{2+} release from the intracellular Ca^{2+} stores contributes to the NMDA-triggered neuronal apoptosis. On the other hand, it also suggests a possibility that in cultured CGNs, Ca^{2+} -induced Ca^{2+} release triggered by NMDA is caused predominantly by IP3R channel opening, while RyR channels may be not opened in or not respond to NMDA stimulation. This hypothesis is supported by these reports presenting that both NMDAR and downstream IP3R activation participates in increasing intracellular Ca^{2+} transients in cortical pyramidal neurons (Nakata & Nakamura 2007), and that cytokine IL-10 modulates Ca^{2+} release induced by NMDAR activation

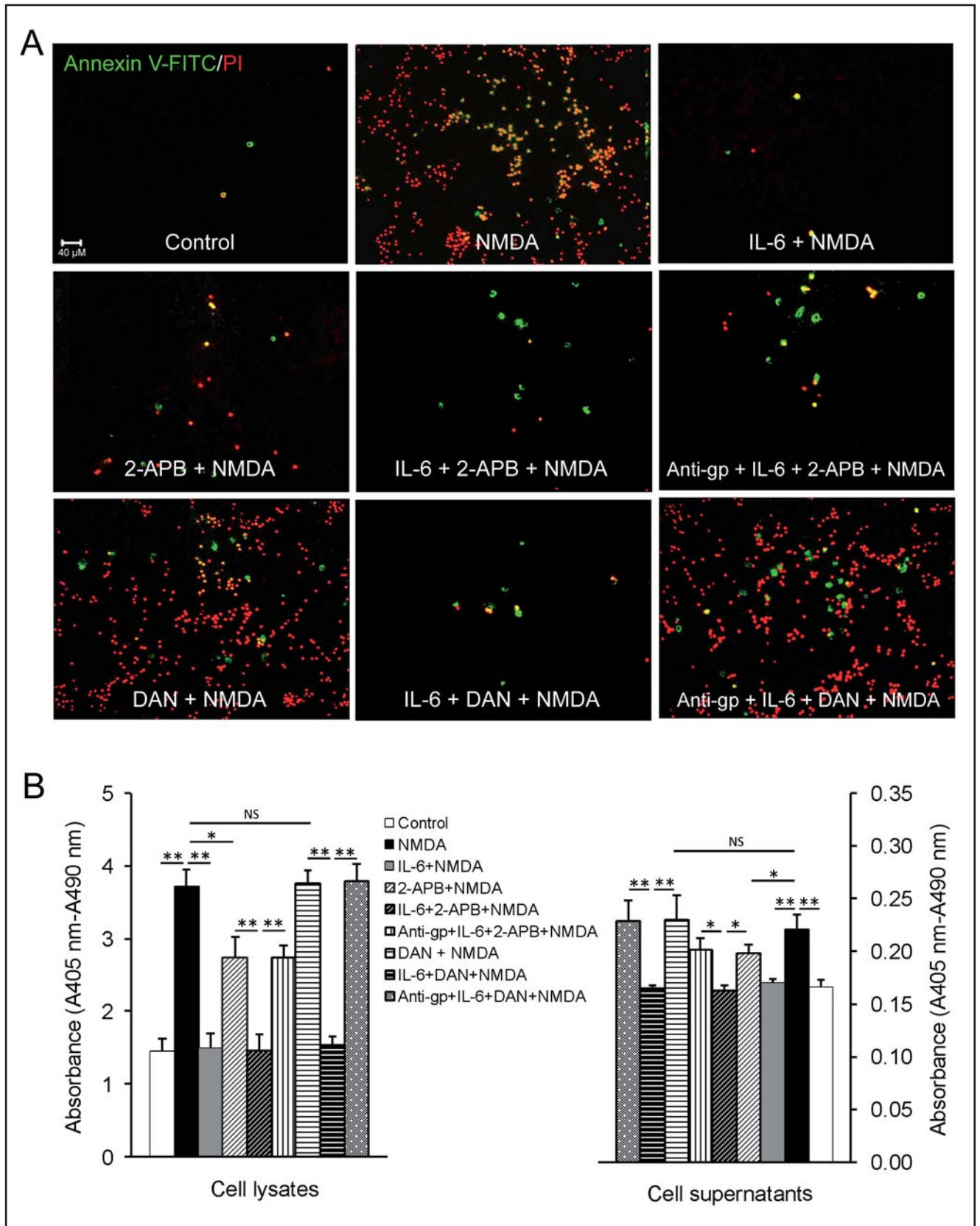


Fig. 3. Effects of IL-6 on NMDA-triggered cell death in 2-APB- or DAN-exposed neurons. The drug treatments of CGNs were the same as designed in figure 1. The annexin V-FITC/PI staining (A) and ELISA (B) were tested at 18 h following NMDA application. (A) A representative image showing apoptotic neurons, stained by annexin V-FITC alone (green) in the plasma membrane, and necrotic cells, labeled throughout the nucleus by PI alone (red) because of losing membrane integrity or by both PI and annexin V-FITC (yellow). (B) A sandwich enzyme immunoassay-based detection of DNA- and histone-associated nucleosomes. The absorbance determined in cell lysates reflects neuronal apoptosis, and the absorbance measured in cell supernatants indicates neuronal necrosis. The data were obtained from five-repeated experiments. * $p < 0.05$, ** $p < 0.01$, and NS no significance between the compared groups.

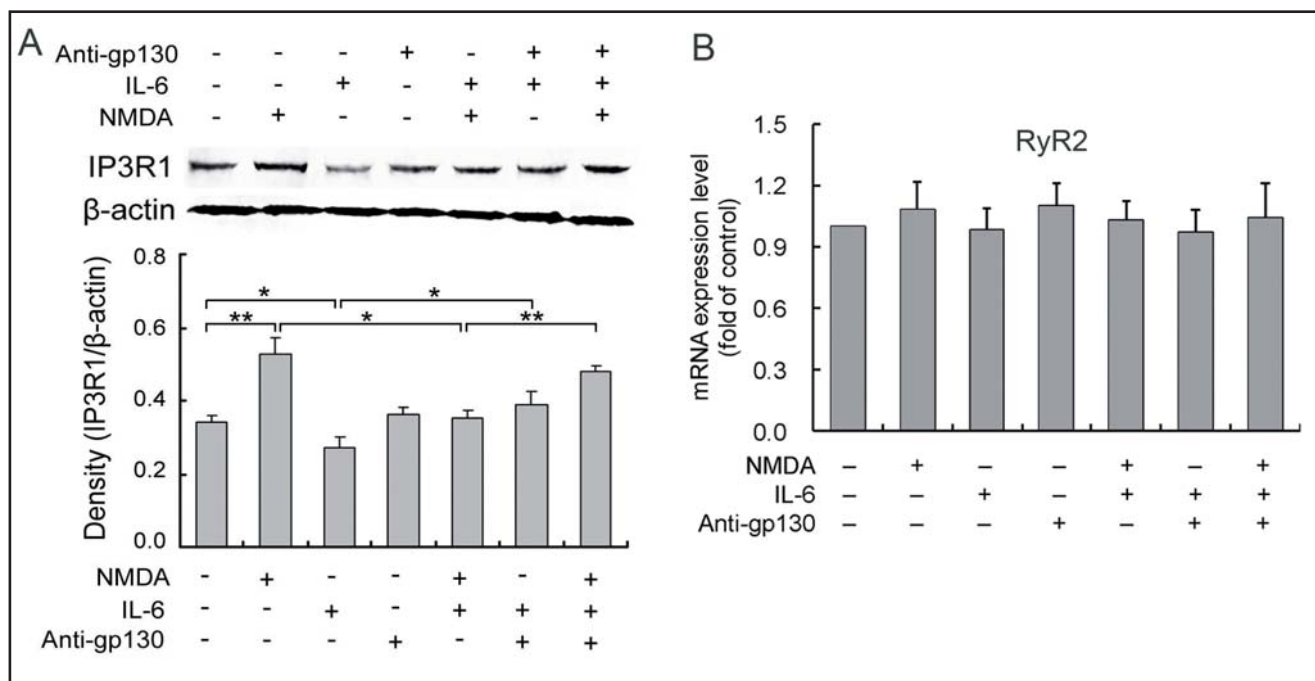


Fig. 4. Changes in IP3R1 and RyR2 expression in CGNs exposed to NMDA, IL-6 or anti-gp130 mAb. The drug exposures of CGNs were the same as designed in figure 1. The expression of IP3R1 protein (A) and RyR2 gene (B) was examined at 8 h following NMDA application by Western blot and real-time PCR, respectively. The experiments were replicated for four times. * $p < 0.05$, ** $p < 0.01$, between the compared groups.

through inhibition of IP3- but not ryanodine-sensitive internal stores in hippocampal neurons (Turovskaya *et al.* 2012). Importantly, IL-6 prevented NMDA-induced apoptosis in either 2-APB- or DAN-treated CGNs, but this effect of IL-6 was stronger on DAN-treated neurons than on 2-APB-exposed cells. Since RyR did not contribute to NMDA-evoked intracellular Ca^{2+} overload, as indicated above, the IL-6 inhibition of apoptosis in 2-APB-treated CGNs may explain a suppression of NMDAR-mediated Ca^{2+} influx-induced apoptosis. Altogether, these results suggest that between IP3R and RyR, IL-6 predominantly inhibits IP3R-dependent Ca^{2+} release-induced neuronal apoptosis. Moreover, all the preventive effects of IL-6 were abolished by anti-gp130 mAb, a neutralizing antibody to gp130 that is a signal-transduction subunit of IL-6 receptors. The data on the one hand confirm IL-6 neuroprotective role and on the other hand, reveal that IL-6 receptor-related signaling mediate this neuroprotection. These results are in line with the recent report (Fang *et al.* 2013).

In support these morphologic results, we found that expression and activity of caspase-3, an effector (executioner) caspase in caspase family that are essential in cells for apoptosis, both were elevated by NMDA in cultured CGNs, and that IL-6 prevented this elevation. It demonstrates an anti-apoptotic mechanism of IL-6 via inhibiting caspase-3. Similarly, antagonism of IP3R with 2-APB downregulated NMDA-induced caspase-3 expression and activity, but antagonism of RyR with DAN did not affect the NMDA-stimulated caspase-3

changes, suggesting that RyR in CGNs is not implicated in caspase-3 events. A report presenting that in B lymphocytes, IP3R1 plays a pivotal role in apoptosis and that the increase in $[Ca^{2+}]_i$ during apoptosis is mainly the consequence of IP3R1 cleavage by caspase-3 (Assefa *et al.* 2004) explains the mechanism of apoptosis at the profile of relationship between caspase-3, IP3R and $[Ca^{2+}]_i$. Our present data support this report and also suggest that in neurons, the IP3R-mediated Ca^{2+} release-induced apoptosis is initiated by caspase-3 cascade. Moreover, in agreement with the observations in TUNEL-determined apoptotic cells, the suppressive effect of IL-6 on expression and activity of caspase-3 was larger in DAN-treated neurons than in 2-APB-exposed cells. The results support the mechanism, i.e., via inhibiting caspase-3, IL-6 prevents IP3R-dependent Ca^{2+} release and apoptosis. Likewise, anti-gp130 mAb impeded these IL-6 suppressive effects on caspase-3 expression and activity induced by NMDA. This further demonstrates that IL-6 receptor-related gp130 signaling mediates IL-6 anti-apoptotic action.

Neuronal cell death in NMDA excitotoxicity includes both apoptotic and necrotic cell death. As shown in annexin V-FITC/PI staining, NMDA triggered amounts of neuronal necrosis besides apoptosis in this study. IL-6 dramatically reduced the NMDA-evoked neuronal necrosis. To relatively quantify these changes, DNA- and histone-associated nucleosomes in cultured CGNs were detected by ELISA. The NMDA-induced increase in absorbance in cell supernatants, which represented

neuronal necrosis, was prevented by IL-6. Simultaneously, the NMDA-induced elevation of absorbance in cell lysates, which reflected neuronal apoptosis, was also significantly suppressed by IL-6. Furthermore, 2-APB markedly reduced NMDA-induced neuronal necrosis, shown by both annexin V-FITC/PI staining and nucleosome detection, but DAN did not influence NMDA-induced neuronal necrosis. These data demonstrate that NMDA-evoked neuronal necrosis is not dependent on RyR activity. Notably, the anti-necrotic effect of IL-6 on DAN-treated neurons was larger than on 2-APB-exposed cells. The findings suggest a predominant action of IL-6 on IP3R. These phenomena are identical with those appearing in IL-6 anti-apoptotic effect and therefore, they provide further evidence for the mechanism that by inhibiting IP3R activity, IL-6 prevents NMDA-induced cytosolic Ca²⁺ overload and as a result, neuronal cell necrosis is suppressed. The downregulated expression of IP3R1, an IP3R isoform, and the non-changed expression of RyR2, a RyR isoform, by IL-6 support the observations in neuronal apoptosis and necrosis, and confirm a major inhibitory action of IL-6 on IP3R opening and expression. These effects of IL-6 prevention from neuronal necrosis and IP3R1 upregulation were also counteracted by anti-gp130 mAb, demonstrating that gp130 signaling mediates IL-6 neuroprotection.

In summary, NMDA-triggered Ca²⁺-induced Ca²⁺ release-mediated apoptosis and necrosis in CGNs predominantly depend on IP3R channel opening and expression rather than RyR activity. IL-6 prevents the IP3R-dependent neuronal apoptosis and necrosis and also may reduce NMDAR-mediated cell apoptosis and necrosis. The prevention from NMDA-induced IP3R1 upregulation by IL-6 and the non-altered RyR2 expression in these drug exposures support a major contribution of IP3R inhibition to IL-6 anti-apoptosis and anti-necrosis. These neuroprotective effects of IL-6 resistance to apoptosis and necrosis are mediated by IL-6 receptor-coupled gp130 signaling.

ACKNOWLEDGMENTS

This study was supported by National Basic Research Program of China (973 Program, No. 2013CB967500) and National Natural Science Foundation of China (No. 81170855 and No. 81070743).

REFERENCES

- Arundine M, Tymianski M (2003). Molecular mechanisms of calcium-dependent neurodegeneration in excitotoxicity. *Cell Calcium*. **34**: 325–337.
- Assefa Z, Bultynck G, Szlufcik K, Nadif Kasri N, Vermassen E, Goris J, Missiaen L, Callewaert G, Parys JB, De Smedt H (2004). Caspase-3-induced truncation of type 1 inositol trisphosphate receptor accelerates apoptotic cell death and induces inositol trisphosphate-independent calcium release during apoptosis. *J Biol Chem*. **279**: 43227–43236.
- Bano D, Nicotera P (2007). Glutamate-Independent Calcium Toxicity: Introduction of Ca²⁺ Signals and Neuronal Death in Brain Ischemia. *Stroke*. **38**: 674–676.
- Cucchiaroni ML, Viscomi MT, Bernardi G, Molinari M, Guatteo E, Mercuri NB (2010). Metabotropic glutamate receptor 1 mediates the electrophysiological and toxic actions of the cycad derivative beta-N-Methylamino-L-alanine on substantia nigra pars compacta DAergic neurons. *J Neurosci*. **30**: 5176–5188.
- Dalla Libera AL, Regner A, de Paoli J, Centenaro L, Martins TT, Simon D (2011). IL-6 polymorphism associated with fatal outcome in patients with severe traumatic brain injury. *Brain Injury*. **25**: 365–369.
- Erta M, Quintana A, Hidalgo J (2012). Interleukin-6, a major cytokine in the central nervous system. *Int J Biol Sci*. **8**: 1254–1266.
- Fang XX, Jiang XL, Han XH, Peng YP, Qiu YH (2013). Neuroprotection of interleukin-6 against NMDA-induced neurotoxicity is mediated by JAK/STAT3, MAPK/ERK, and PI3K/AKT signaling pathways. *Cell Mol Neurobiol*. **33**: 241–251.
- Fernandez-Gomez FJ, Gomez-Lazaro M, Pastor D, Calvo S, Aguirre N, Galindo MF, Jordan J (2005). Minocycline fails to protect cerebellar granular cell cultures against malonate-induced cell death. *Neurobiol Dis*. **20**: 384–391.
- Frei K, Leist TP, Meager A, Gallo P, Leppert D, Zinkernagel RM, Fontana A (1988). Production of B cell stimulatory factor-2 and interferon gamma in the central nervous system during viral meningitis and encephalitis. Evaluation in a murine model infection and in patients. *J Exp Med*. **168**: 449–453.
- Gadient RA, Otten U (1993). Differential expression of interleukin-6 (IL-6) and interleukin-6 receptor (IL-6R) mRNAs in rat hypothalamus. *Neurosci Lett*. **153**: 13–16.
- Gadient RA, Otten U (1994). Identification of interleukin-6 (IL-6)-expressing neurons in the cerebellum and hippocampus of normal adult rats. *Neurosci Lett*. **182**: 243–246.
- Galiano M, Liu ZQ, Kalla R, Bohatschek M, Koppius A, Gschwendner A, Xu S, Werner A, Kloss CU, Jones LL, Bluethmann H, Raivich G (2001). Interleukin-6 (IL6) and cellular response to facial nerve injury: effects on lymphocyte recruitment, early microglial activation and axonal outgrowth in IL6-deficient mice. *Eur J Neurosci*. **14**: 327–341.
- Gruol DL, Netzeband JG, Nelson TE (2010). Somatic Ca²⁺ signaling in cerebellar Purkinje neurons. *J Neurosci Res*. **88**: 275–289.
- Hama T, Miyamoto M, Tsukui H, Nishio C, Hatanaka H (1989). Interleukin-6 as a neurotrophic factor for promoting the survival of cultured basal forebrain cholinergic neurons from postnatal rats. *Neurosci Lett*. **104**: 340–344.
- Hama T, Kushima Y, Miyamoto M, Kubota M, Takei N, Hatanaka H (1991). Interleukin-6 improves the survival of mesencephalic catecholaminergic and septal cholinergic neurons from postnatal, two-week-old rats in cultures. *Neuroscience*. **40**: 445–452.
- Inomata Y, Hirata A, Yonemura N, Koga T, Kido N, Tanihara H (2003). Neuroprotective effects of interleukin-6 on NMDA-induced rat retinal damage. *Biochem Biophys Res Commun*. **302**: 226–232.
- Klein MA, Möller JC, Jones LL, Bluethmann H, Kreutzberg GW, Raivich G (1997). Impaired neuroglial activation in interleukin-6 deficient mice. *Glia*. **19**: 227–233.
- Laurenzi MA, Sidén A, Persson MA, Norkrans G, Hagberg L, Chiodi F (1990). Cerebrospinal fluid interleukin-6 activity in HIV infection and inflammatory and noninflammatory diseases of the nervous system. *Clin Immunol Immunopathol*. **57**: 233–241.
- Liu Z, Qiu YH, Li B, Ma SH, Peng YP (2011). Neuroprotection of interleukin-6 against NMDA-induced apoptosis and its signal-transduction mechanisms. *Neurotox Res*. **19**: 484–495.
- Mendonça Torres PM, de Araujo EG (2001). Interleukin-6 increases the survival of retinal ganglion cells in vitro. *J Neuroimmunol*. **117**: 43–50.
- Monje ML, Toda H, Palmer TD (2003). Inflammatory blockade restores adult hippocampal neurogenesis. *Science*. **302**: 1760–1765.
- Nakanishi M, Niidome T, Matsuda S, Akaike A, Kihara T, Sugimoto H (2007). Microglia-derived interleukin-6 and leukaemia inhibitory factor promote astrocytic differentiation of neural stem/progenitor cells. *Eur J Neurosci*. **25**: 649–658.

- 23 Nakata H, Nakamura S (2007). Brain-derived neurotrophic factor regulates AMPA receptor trafficking to post-synaptic densities via IP3R and TRPC calcium signaling. *FEBS Lett.* **581**: 2047–2054.
- 24 Penkowa M, Giralt M, Carrasco J, Hadberg H, Hidalgo J (2000). Impaired inflammatory response and increased oxidative stress and neurodegeneration after brain injury in interleukin-6-deficient mice. *Glia.* **32**: 271–285.
- 25 Penkowa M, Giralt M, Lago N, Camats J, Carrasco J, Hernández J, Molinero A, Campbell IL, Hidalgo J (2003). Astrocyte-targeted expression of IL-6 protects the CNS against a focal brain injury. *Exp Neurol.* **181**: 130–148.
- 26 Peng YP, Qiu YH, Lu JH, Wang JJ (2005). Interleukin-6 protects cultured cerebellar granule neurons against glutamate-induced neurotoxicity. *Neurosci Lett.* **374**: 192–196.
- 27 Popescu AT, Saghyan AA, Nagy FZ, Paré D (2010). Facilitation of corticostriatal plasticity by the amygdala requires Ca^{2+} -induced Ca^{2+} release in the ventral striatum. *J Neurophysiol.* **104**: 1673–1680.
- 28 Schöbitz B, Voorhuis DA, De Kloet ER (1992). Localization of interleukin 6 mRNA and interleukin 6 receptor mRNA in rat brain. *Neurosci Lett.* **136**: 189–192.
- 29 Schöbitz B, de Kloet ER, Sutanto W, Holsboer F (1993). Cellular localization of interleukin 6 mRNA and interleukin 6 receptor mRNA in rat brain. *Eur J Neurosci.* **5**: 1426–1435.
- 30 Spooren A, Kolmus K, Laureys G, Clinckers R, De Keyser J, Haegeman G, Gerlo S (2011). Interleukin-6, a mental cytokine. *Brain Res Rev.* **67**: 157–183.
- 31 Sun XM, Lu JH, Qiu YH, Liu Z, Wang XQ, Peng YP (2011). Interleukin-6 reduces NMDA-induced Ca^{2+} overload via prevention of Ca^{2+} release from intracellular store. *Int J Neurosci.* **121**: 423–429.
- 32 Suzuki S, Tanaka K, Suzuki N (2009). Ambivalent aspects of interleukin-6 in cerebral ischemia: inflammatory versus neurotrophic aspects. *J Cereb Blood Flow Metab.* **29**: 464–479.
- 33 Swartz KR, Liu F, Sewell D, Schochet T, Campbell I, Sandor M, Fabry Z (2001). Interleukin-6 promotes post-traumatic healing in the central nervous system. *Brain Res.* **896**: 86–95.
- 34 Turovskaya MV, Turovsky EA, Zinchenko VP, Levin SG, Godukhin OV (2012). Interleukin-10 modulates $[Ca^{2+}]_i$ response induced by repeated NMDA receptor activation with brief hypoxia through inhibition of InsP(3)-sensitive internal stores in hippocampal neurons. *Neurosci Lett.* **516**: 151–155.
- 35 Vallières L, Campbell IL, Gage FH, Sawchenko PE (2002). Reduced hippocampal neurogenesis in adult transgenic mice with chronic astrocytic production of interleukin-6. *J Neurosci.* **22**: 486–492.
- 36 Verkhatsky A, Petersen OH (2002). The endoplasmic reticulum as an integrating signaling organelle: from neuronal signaling to neuronal death. *Eur J Pharmacol.* **447**: 141–154.
- 37 Wang XQ, Peng YP, Lu JH, Cao BB, Qiu YH (2009). Neuroprotection of interleukin-6 against NMDA attack and its signal transduction by JAK and MAPK. *Neurosci Lett.* **450**: 122–126.
- 38 Won SJ, Kim DY, Gwag BJ (2002). Cellular and Molecular Pathways of Ischemic Neuronal Death. *J Biochem Mol Biol.* **35**: 67–86.